ELSEVIER

Journal of Nuclear Materials 290–293 (2001) 551–555

journal of nuclear materials

www.elsevier.nl/locate/jnucmat

Study of the relation between density and temperature fall-off lengths in a detached divertor plasma

K. Borrass *

Max-Plank-Institut für Plasmaphysik, Euratom Association, Postfach 1533, 85740 Garching, Germany

Abstract

Theory has shown that completely detached gas targets are completely controlled by the transverse ion–neutral collisionality. In order to transform this information to a format of practical relevance, knowledge of the plasma density width Δ_n^* at the gas target entrance (GTE) is required. In a previous work, Δ_n^* was determined with the relation $\Delta_n^* \propto \Delta_T$, where Δ_T is the upstream temperature fall-off length, which can be reliably estimated. This paper provides evidence for this relation, which is not a priori obvious. In the absence of empirical data, one has to rely on a computational (B2-EIRENE) database. Proportionality between Δ_n^* and Δ_T is confirmed. Complementary analytical considerations are presented to elucidate the underlying physics.

Keywords: SOL plasma; Detached plasma

1. Introduction

Understanding divertor detachment has been one of the major achievements in edge physics in the past decade. A specific interest in well-detached divertor plasmas arises through the intimate link with density limits [1,2] and the power exhaust problem [3]. Most studies of detachment have relied on 2-D simulation codes, but despite the complexity of detached scrape-off layer plasmas, some progress has been made in the analytical treatment [1]. This study is devoted to a special aspect of this approach.

The way the gas target is experienced by the upstream plasma is characterized by the two dimensionless parameters $\gamma^* = q_\parallel^*/(n^* T^* c_s^*(T^*)$ and $M^* = \Gamma^*/\ (n^* c_s^*(T^*))$, where * indicates quantities at the gas target entrance (GTE), $q_\parallel$ the parallel heat flux, n the ion density, T the temperature ($T_e \simeq T_i \equiv T$), and c_s is the ion sound speed. M^* is the Mach number at the GTE, while γ^* is a kind of generalized sheath transmission coefficient. The key result of [1] is that γ^* and M^* depend only on the transverse ion–neutral collisionality $\Delta_n^*/\lambda_{i\text{-}n}^*$ at the GTE

$$\gamma^* = \gamma^*\left(\frac{\Delta_n^*}{\lambda_{i\text{-}n}^*}\right), \qquad M^* = M^*\left(\frac{\Delta_n^*}{\lambda_{i\text{-}n}^*}\right), \tag{1}$$

where Δ_n^* and $\lambda_{i\text{-}n}^* = 1/(n^*\sigma_{i-n})$ are, respectively, the plasma density width and the ion–neutral mean free path at the GTE. σ_{i-n} is the ion–neutral (elastic and charge exchange) cross-section ($\sigma_{i-n} \simeq$ const).

In order to draw conclusions of practical relevance from Eq. (1), one has to translate it into a form where quantities such as the upstream plasma density and temperature, the power into the SOL, etc. replace GTE quantities. This is achieved by applying the standard two-point model [1] to the region between the GTE and the stagnation point, with the relations of Eq. (1) being used as boundary conditions at the GTE. This approach requires knowledge of Δ_n^*. Reliable estimates exist for the upstream temperature fall-off length Δ_T, which is basically determined by the competition of parallel (Spitzer type) and (anomalous) perpendicular heat transport in an essentially source-free region [4]. The plasma density shape in the SOL, on the other hand, is largely determined by sources which show a complex spatial distribution and the strength of which is not simply determined by externally controllable parameters. According to common thinking, one would therefore not expect simple estimates to exist for Δ_n^*. In [1], this problem was circumvented by the assumption

* Tel.: +49-89 3299 1844; fax: +49-89 3299 1844.
E-mail address: kurt.borrass@ipp.mpg.de (K. Borrass).

0022-3115/01/$ - see front matter
PII: S0022-3115(00)00592-4

$$\Delta_n^* \propto \Delta_T. \quad (2)$$

Though some evidence of the validity of this relation was presented, it is actually not particularly obvious. This study is dedicated to a more in-depth justification of Eq. (2). While empirical information on fall-off lengths in the upstream and near-target regions exists (see, for instance, [5,6]), no data is available for the GTE region, which is typically located near the *X*-point. One thus has to rely on 2-D simulations.

2. Numerical database

The relation between Δ_n^* and Δ_T is checked against a numerical database of completely detached (drop of the particle flux to the target by at least one order of magnitude) B2-EIRENE solutions that were obtained for a JET MARK-I divertor configuration. This choice was entirely determined by practical considerations since most of the runs were available from previous studies. Actually, divertor geometry effects are not expected to be relevant to the questions under discussion. For similar reasons, all cases are pure hydrogen cases. Most runs rely on constant transverse heat and particle transport ($\chi_\perp$, $D_\perp = const$), but a few cases with Bohm-type transport are also included. The input power P_{in}, safety factor q_ψ, and (in the case of Bohm-type transport) toroidal field B_t are the the dominant parameters that control a discharge. (See Table 1.) Note that, with the requirement of complete detachment imposed, one degree of freedom is lost and one is no longer free to choose the particle content (or any other equivalent parameter such as the gas rate) in addition.

3. 2-D aspects of completely detached solutions and definition of fall-off lengths

Completely detached solutions show a characteristic shift of the ionization zone into off-separatrix regions, leading to an off-separatrix density peak which actually defines the density width at the GTE (see Figs. 1 and 2). This suggests the definitions of Δ_T and Δ_n^* according to Fig. 3. A complication arises through the 2-D aspects of the ionization zone and in particular its considerable poloidal/vertical extent. In B2-EIRENE, vertical positions are naturally characterized by the poloidal grid

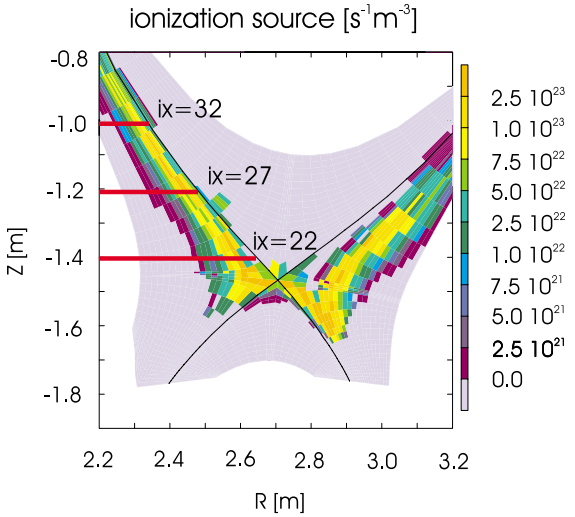

Fig. 1. Shape of the ionization zone in the *Z*–*R* plane. *Z* is the vertical position, while *R* is the distance from the symmetry axis.

Table 1
Range of parameters covered by the database[a]

Run	P_{in} (MW)	q_{95}	B_t (T)	Δ_n^* (cm)	Δ_T (cm)	T_S (eV)
R-09[b]	1.8	3.6	2.4	26.0[c]	14.0	32.2
R-12[b]	2.4	3.6	2.4	24.0	10.1	44.5
R-18[b]	3.6	3.6	2.4	20.0	7.83	53.8
R-12HQ[b]	2.4	5.4	2.4	20.5	8.83	58.5
R-12LQ[b]	2.4	2.4	2.4	27.7	10.7	27.4
R-18HQ[b]	3.6	5.4	2.4	19.5	7.2	72.6
R-18LQ[b]	3.6	2.4	2.4	25.0	9.2	38.6
R-09HQ[b]	1.8	5.4	2.4	29.5	10.5	48.1
R-12B[d]	2.4	3.6	2.4	24.5	10.0	45.0
R-12LB[d]	2.4	3.6	1.6	34.5	12.0	43.5
R-12HB[d]	2.4	3.6	3.6	21.5	8.5	47.5

[a] B_t, q_{95}, and P_{in} are the toroidal field, safety factor, and input power, respectively. Δ_n^* and Δ_T are as defined in the text. T_S is the upstream separatrix temperature.
[b] Constant transport.
[c] See Section 4.
[d] Bohm-type diffusion.

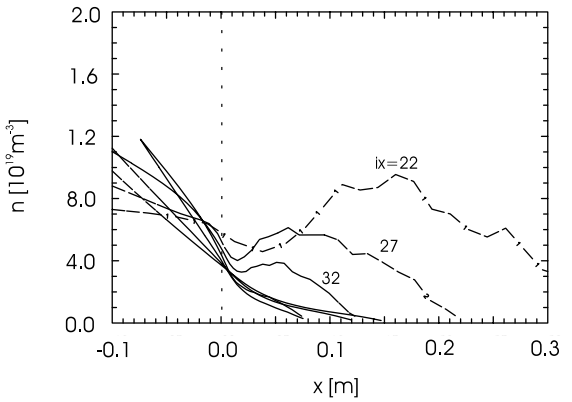

Fig. 2. Plasma density versus x (distance from the separatrix) for various positions (inboard divertor). An off-separatrix density blob is formed at the GTE.

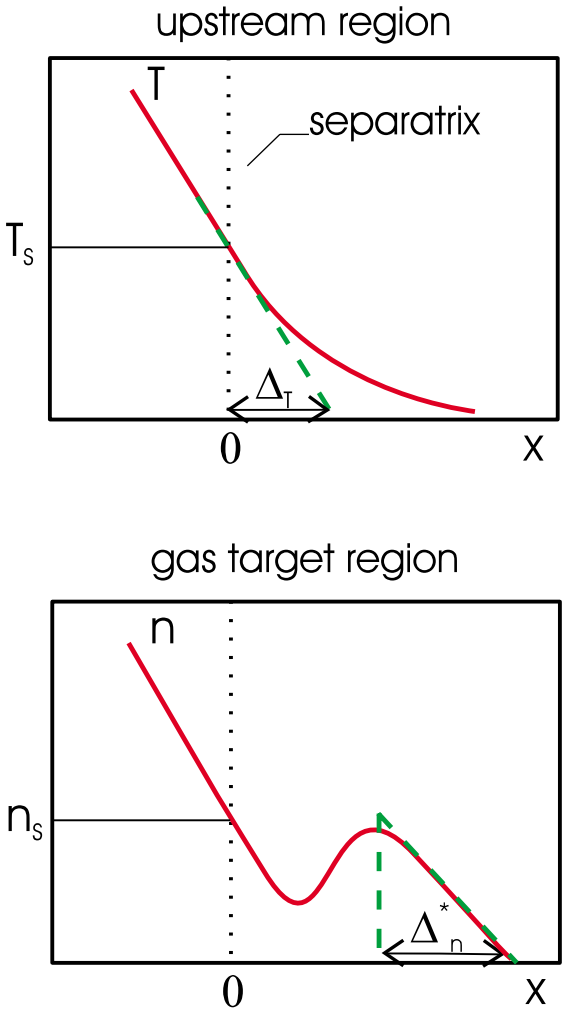

Fig. 3. Definition of upstream temperature fall-off length Δ_T and GTE density width Δ_n^* as suggested by the previous discussion.

label ix ($ix = 1$–92 in the present case). We are mainly interested in scaling relations which are virtually independent of the particular vertical position at which GTE quantities are considered. In what follows, we take data at $ix = 22$ (see Fig. 1) and $ix = 46$ (top position) to determine GTE and upstream quantities, respectively.

4. Validation of scaling assumptions

In Fig. 4, Δ_T is plotted versus Δ_n^*. The relation $\Delta_n^* \propto \Delta_T$ is indeed quite well satisfied, except for the low q_ψ, low P_{in} case R-09, which was not included. In this very low-density case the ionization peak moves inside the separatrix and the ionization-induced density blob merges with the proper density scrape-off layer, making the definition of Δ_n^* according to Fig. 3 dubious.

5. Analytical interpretation

We are not able to provide a rigorous analytical derivation of Eq. (2). However, it may prove useful to complement our numerical efforts by some heuristic considerations that provide better insight into the underlying physics. Many of the notations used in this section are illustrated in Fig. 5.

We describe the upstream SOL within a slab geometry with coordinates z (distance along field lines) and x (distance from the separatrix). Thus, in general, $n = n(z,x)$ and $T = T(z,x)$. By Definition $z = 0$ in the stagnation point, so that the upstream (stagnation point) separatrix density n_S and separatrix temperature T_S are given by $n_S = n(0,0)$ and $T_S = T(0,0)$, respectively.

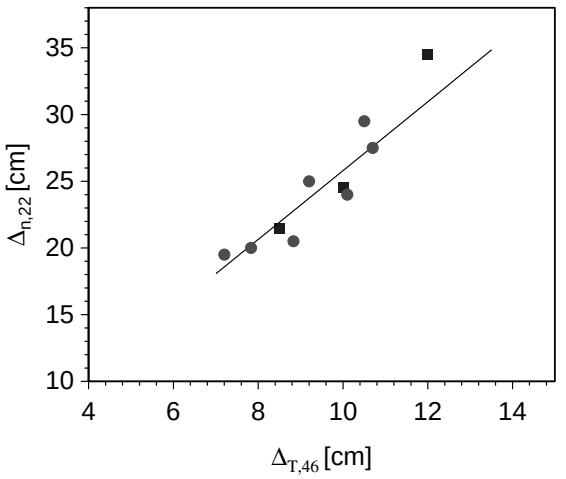

Fig. 4. Δ_n^* versus Δ_T, with Δ_n^* and Δ_T represented by $\Delta_{n,22}$ and $\Delta_{T,46}$, respectively. Bullets: $D_\perp = \text{const}$. Squares: cases with Bohm-type perpendicular transport.

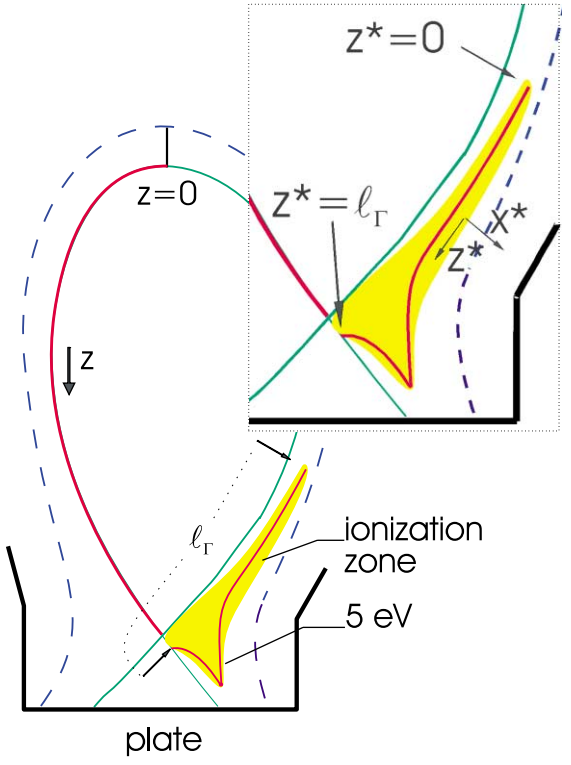

Fig. 5. Illustration of notations and coordinates used in Section 5.

Continuity of the transverse power flux at the separatrix results in the usual estimate of the upstream temperature fall-off length Δ_T at the separatrix [4] ($q_\perp$ is the mean power flux across the separatrix and B_t is the toroidal field)

$$\Delta_T \propto \frac{n_S T_S}{q_\perp} \tag{3}$$

in the case of constant transverse heat diffusivity and

$$\Delta_T \propto \frac{n_S T_S^2}{q_\perp B_t} \tag{4}$$

in the case of Bohm-type transport.

The ionization source is strongly peaked at a constant temperature T^* of about 5 eV [1]. We model the vicinity of the 5 eV contour by a slab with coordinates z^* (distance along the 5 eV contour) and x^* (radial distance from the 5 eV contour) and length ℓ_Γ. $z^* = 0$ at the upstream end of the ionization zone by definition (see Fig. 5). We now integrate the steady-state version of the particle balance ($\nabla\vec{\Gamma} = S$, where $\vec{\Gamma}$ is the particle flux and S is the particle source/sink) over the rectangle that just encloses the ionization zone, i.e., over the region $[0 \leqslant z^* \leqslant \ell_\Gamma]$, $[-\delta/2 \leqslant x^* \leqslant +\delta/2]$, where δ characterizes the radial width of the ionization zone. With $S_\Gamma = 1/\ell_\Gamma \int_0^{\ell_\Gamma} dz^* \int_{-\delta/2}^{+\delta/2} dx^* S_{ion}(z^*, x^*)$, where S_{ion} is the ionization rate, we get

$$\begin{aligned} S_\Gamma &\simeq 1/\ell_\Gamma \int_0^{\ell_\Gamma} dz^* \int_{-\delta/2}^{+\delta/2} dx^* \nabla\vec{\Gamma} \\ &\simeq 1/\ell_\Gamma \int_0^{\ell_\Gamma} dz^* (\Gamma_{x^*}(z^*, +\delta/2) - \Gamma_{x^*}(z^*, -\delta/2)) \\ &\simeq 1/\ell_\Gamma \int_0^{\ell_\Gamma} dz^* \left(\frac{D_\perp(z^*, +\delta/2) n^*(z^*, +\delta/2)}{\Delta_n^*(z^*, \delta/2)} \right. \\ &\quad \left. + \frac{D_\perp(z^*, -\delta/2) n^*(z^*, -\delta/2)}{\Delta_n^*(z^*, -\delta/2)} \right), \end{aligned} \tag{5}$$

where Γ_{x^*} is the x^* component of the particle flux, $D_\perp^*(z^*, x^*)$ the transverse diffusivity, $n^*(z^*, x^*)$ the plasma density and $\Delta_n^*(z^*, x^*)$ is the local density fall-off length. In going to the second line of Eq. (5) terms of order $\delta/\ell_\Gamma \ll 1$ were neglected.

Due to the radial localization of the ionization zone $n^*(z^*, +\delta/2) \simeq n^*(z^*, -\delta/2) \simeq n^*(z^*, 0)$ and $D_\perp(z^*, +\delta/2) \simeq D_\perp(z^*, -\delta/2) \simeq D_\perp(z^*, 0)$. For the transport models under consideration (no density dependence) $D_\perp(z^*, 0) \equiv D_\perp$, independent of z^*. Also, the simulations suggest $\Delta_n^*(z^*, +\delta/2) \simeq \Delta_n^*(z^*, -\delta/2)$ (see Fig. 2). Hence

$$S_\Gamma \simeq 2 D_\perp^* \frac{1}{\ell_\Gamma} \int dz^* \frac{n^*(z^*, 0)}{\Delta_n^*(z^*, 0)} \propto \frac{n^*(\ell_\Gamma)}{\Delta_n^*}. \tag{6}$$

In writing down the second part of (6), typical shapes (with respect to z^*) of $n^*(z^*, 0)$ and $\Delta_n^*(z^*, 0)$ are in addition assumed to exist so that we can characterize them by $n^*(\ell_\Gamma, 0)$ and any particular Δ_n^*, respectively. A simple density shape as exhibited by the simulations (see Fig. 2) is mandatory to make this approach meaningful.

Constant pressure along B and $T^* \simeq$ const implies

$$n^*(\ell_\Gamma, 0) \propto n^*(\ell_\Gamma, 0) T^* \propto n_S T_S. \tag{7}$$

It thus follows that

$$\Delta_n^* \propto \frac{n_S T_S}{S_\Gamma} \tag{8}$$

for constant $D_\perp$ and

$$\Delta_n^* \propto \frac{n_S T_S}{B_t S_\Gamma} \tag{9}$$

for Bohm-type transverse diffusion.

In order to obtain a relation like Eq. (2), $q_\perp \propto S_\Gamma$ must obviously hold. The energy balance in a flux tube reads

$$q_\perp L_X (1 - f_{rad}^{SOL})(1 - f_E) \simeq S_\Gamma \ell_\Gamma \xi + Q_t, \tag{10}$$

where L_X is the connection length between the stagnation point and X-point, f_{rad}^{SOL} the SOL impurity radiative fraction, f_E the fraction of the power entering the recycling zone that is lost through $i - n$ interaction and ξ is the energy cost per ionization. Q_t is the target heat load.

$\xi \simeq$ const is a reasonable approximation. In low-temperature detached SOL plasmas, we have in addition $S_\Gamma \ell_\Gamma \xi \gg Q_t$ and $f_E \ll 1$ [3]. With complete detachment, there is thus a simple relation between the power input to the SOL and the total number of ionization events per second

$$q_\perp L_X (1 - f_{rad}^{SOL}) \propto S_\Gamma \ell_\Gamma.$$

One thus gets

$$\frac{\Delta_n^*}{\Delta_T} \propto \frac{q_\perp}{S_\Gamma} \propto \frac{\ell_\Gamma}{(1 - f_{rad}^{SOL}) L_X} \propto \frac{1}{(1 - f_{rad}^{SOL})}, \tag{11}$$

$$\frac{\Delta_n^*}{\Delta_T} \propto \frac{1}{(1 - f_{rad}^{SOL}) T_S} \tag{12}$$

for constant and Bohm-type transport, respectively, if it is assumed that ℓ_Γ / L_X is a constant. This is the least obvious assumption made in this section. An essential ingredient is that neutrals, born at the plate or near the plate by volume recombination, leave the SOL plasma radially and reach the ionization zone by travelling outside the SOL [3]. This a diffusive type of process, where the neutral bounces between chamber walls and plasma. In order that the neutral is reflected by the plasma instead of being absorbed, a number of collisions (elastic or charge exchange) have to be performed before the neutral may reach the 5 eV contour. This requires that a region exists (in radial direction) where $\nu_{ion} \ll \nu_{collision}$, where ν_{ion} and $\nu_{collision}$ are, respectively, the ionization and (elastic and charge exchange) collision frequencies. In view of the typical density and temperature distribution in the SOL and the temperature and density dependencies of ν_{ion} and $\nu_{collision}$, it is easy to see that this condition cannot be fulfilled above a certain poloidal position which defines the upper end of the ionization zone. In our simulations, we find that this position is rather stiff and largely independent of the parameter variations. However, it cannot be excluded that the chamber and divertor geometry, fixed in our study, may have some impact. A more detailed analysis of this aspect is beyond the scope of the present paper.

The arguments that led to Eqs. (11) and (12) can easily be extended to other transport scalings. In general, one would expect for a scaling of the form $D_\perp,\ \chi_\perp \propto n^\alpha T^\beta$ that

$$\frac{\Delta_n^*}{\Delta_T} \propto \frac{1}{(1 - f_{rad}^{SOL}) T_S^{\beta - \alpha}}. \tag{13}$$

Unfortunately, the temperature variation in the subset of the Bohm runs of Table 1 is too modest to check this effect.

6. Summary and conclusions

On the basis of 2-D simulations, it has been shown that $\Delta_n^* \propto \Delta_T$ holds for completely detached discharges which are governed by constant transverse transport. Complementary analytical considerations reveal that the proportionality between the net input power and total ionization rate, valid with complete detachment, is a key element. They also indicate that an additional temperature dependence may arise in the relation between Δ_n^* and Δ_T in the presence of more complex transport scalings. This issue requires further investigation.

In highly detached solutions, the ionization zone is shifted into off-separatrix regions and forms a high-density blob, typically at the X-point height. Material structures in this region would almost certainly affect our results and this may constitute an additional channel for divertor geometry effects.

References

[1] K. Borrass, R. Schneider, R. Farengo, Nucl. Fus. 37 (1997) 523.
[2] K. Borrass, J. Lingertat, R. Schneider, Contrib. Plasma Phys. 38 (1998) 130.
[3] K. Borass, in: S. Kuhn, T. Rognlien (Eds.), in: Proceedings of the Edge-Plasma Theory and Simulation Workshop, Innsbruck, Austria, 6–8 July 1998, Czech. J. Phys., vol 48 (Suppl. S2) (1998) 113.
[4] K. Borass, Nucl. Fus. 31 (1991) 1035.
[5] S.K. Erents, P.C. Stangeby, Nucl. Fus. 38 (1998) 1637.
[6] S.K. Erents, P.C. Stangeby, B. La Bombard, J.D. Elder, W. Fundamenski, Nucl. Fus. 40 (2000) 309.